Int J Adv Manuf Technol (2013) 69:1547–1556
DOI 10.1007/s00170-013-5124-5

ORIGINAL ARTICLE

Multiobjective optimization design of porthole extrusion die using Pareto-based genetic algorithm

Guoqun Zhao · Hao Chen · Cunsheng Zhang · Yanjin Guan

Received: 15 April 2012 / Accepted: 10 June 2013 / Published online: 27 June 2013

Abstract The extrusion die plays a crucial role in aluminum alloy profile production, which influences product quality and service life of extrusion die directly. In this paper, a profile with irregular shape was taken as an analysis example, and multiobjective optimization for porthole extrusion die based on modern intelligence algorithm was carried out. Aiming at achieving the uniform velocity distribution in the cross-section of the profile as well as decreasing the maximum stress on the extrusion die and the deflection of the mandrel, the angle between port bridges, the position of die orifice, and the height of welding chamber were considered as the design variables. Then Kriging model was established on the basis of Latin hypercube samplings, and above design variables were optimized using Pareto-based genetic algorithm. Finally, an optimal die structure is gained. Compared with the initial scheme, the velocity distribution in the extrudate was more even, and the stress on the die and the deflection of the mandrel were decreased obviously in the optimal scheme. The optimal design method for porthole die has strong commonality, thus, it could give useful guidelines for practical production of the same kind of aluminum profile.

Keywords Extrusion · Multiobjective optimization · Kriging model · Genetic algorithm

G. Zhao · H. Chen (✉) · C. Zhang · Y. Guan
Key Laboratory for Liquid–solid Structural Evolution and Processing of Materials (Ministry of Education), Shandong University, Jinan, Shandong 250061, People's Republic of China
e-mail: chenhao1984223@163.com

H. Chen
Inner Mongolia Electric Power Science Research Institute, Hohhot, Inner Mongolia 010020, People's Republic of China

1 Introduction

Hollow aluminum profile has been widely used in many fields in recent years, such as civil architecture, traffic transportation, aviation, aerospace, and communication, etc., mainly because of its characteristic of high strength–weight ratio, good dimensional accuracy, and ease of recycling [1].

In practice, aluminum hollow sections are usually produced using a conventional direct extrusion press and a porthole die [2]. During the flat porthole die extrusion, the high-temperature billet metal is split into distinct streams by port bridges. Then, these metal streams are gathered in the welding chamber, and the soften metal is finally extruded out through the shaped orifice of the die as a fully formed profile [3].

Usually, the extrusion process is a nonlinear one with large deformation, high-temperature, high pressure, and high friction, thus the flow behavior of material and status of die stress are difficult to investigate by means of traditional measurement techniques. While using numerical simulation, the information of die stress state, velocity distribution in the aluminum profile, and extrusion load could be gained. Thus, the potential defects of the product could be found. Importantly, the process parameters and die structure can be optimized by using numerical simulation-based optimization methods before the die is manufactured. Therefore, the numerical simulation can shorten the die design cycle and reduce the production cost. It is also important for improving the quality of the profile and prolonging the service life of extrusion die.

In recent years, more and more studies on the numerical simulation of extrusion process have been carried out. These numerical models are used to investigate the effects of process and die structure parameters on the product quality and the service life of extrusion die. Mehtaa analyzed the extrusion process of an I-shape product using 12 different die

shapes and found that shear dies with feeder plates could have the same flow characteristics but better surface finish in comparison with streamlined dies [4]. Wu simulated the extrusion process of an aluminum AA1100 rectangular hollow pipe using finite volume method and found that the path shape from the portholes to the bearing entrance was an important parameter in flat porthole die design [5]. Chen studied the effects of the process parameters, such as extrusion temperature, extrusion speed, dimensions of billet, and location of holes on the load and the shape of extruded tubes for multi-hole extrusion process by the finite element analysis [6]. Zhang investigated the effects of process parameters on extrusion process and gained optimum combination of process parameters based on Taguchi's method with signal-to-noise ratio and analysis of variance [7]. Fang designed a series of single-bearing dies with pockets of different sizes, volumes, and shapes and investigated the effects of pocket geometric parameters on metal flow by means of numerical simulation in combination with experimental verification [8]. Wu proposed a new approach based on finite element method, polynomial network, and genetic algorithm to optimize geometric parameters of extrusion die [9]. Zou optimized the die profile for hot extrusion using updated sequential quadratic programming method, and the results had been validated by real experiment [10]. Li studied the effect of inner cone punch on metal flow in extrusion process [11]. Padmanathan investigated extrusion die parameters such as shape, depth of pocket, location of die hole, and local bearing lengths on the flow behavior during extrusion for both simple and complex geometries [12]. Donati studied the effects of extrusion speed and shape of port bridge on the quality of the weld and proposed a new criteria for evaluating weld quality [13]. Arif studied the effects of ram speed and die profile on extrusion pressure by using dies of different complexity in hot extrusion of AA6063 [14]. Masri outlined a computer system for analyzing and improving the efficiency of aluminum extrusion operations and applied it successfully in practice [15]. Zhang analyzed metal flow behavior at each stage during the whole extrusion process and dead zones in the die cavity by means of arbitrary Lagrangian–Eulerian method [16]. Chitkara proposed an adaptive directional-reduced integration technique and applied it to rigid-plastic finite element analysis of heading and backward extrusion to enhance stability and efficiency of computation [17].

Currently, most investigations are focused on single objective optimization of relatively simple solid or axisymmetric hollow profile, but multiobjective optimization of complex hollow profile extrusion has not much been presented in the literature so far.

In this paper, a profile with irregular shape was taken as an analysis example, and multiobjective optimization was carried out for porthole extrusion die based on modern intelligence algorithm. And the effects of the layout of port bridges, the shape of welding chamber and the position of die orifice on metal flow, and die strength have been investigated. Firstly, the standard deviation of the velocity field (SDV) in the cross-section of the bearing exit, maximum die stress, and mandrel deflection are selected as the estimate targets, and the Latin hypercube method is used to select sample points of die structure design variables. Then, the Kriging model is established with the simulation results. Finally, the Pareto-based genetic algorithm is used to solve the problem of the multiobjective optimization for porthole extrusion die.

2 Die design and numerical simulation model

2.1 Initial die design

Figure 1 shows the main dimensions of the cross-section and the 3D model of profile in the present study. It is a typical industrial profile with the wall thickness of 2 mm, and its section area is 516 mm^2. Figure 2 gives the 3D model of the initial die structure designed for producing the profile. The outer diameter and height of the upper die are 275 and 80 mm, respectively, as shown in Fig. 2a. Three portholes are adopted in the upper die in order to allocate material rationally and balance the metal flow effectively. The width of port bridge is 30 mm, and the angle between port bridges (α) is 45°. Single chamfering is adopted in the port bridges at the bottom of the die in order to control metal flow effectively. Figure 2b shows the 3D model of the lower die, and its outer diameter and the height are 275 and 80 mm, respectively. The height of the welding chamber is 25 mm, and the distance between the bottom edge of die orifice and the extrusion center (L) is 20 mm. In addition, there is a two-step run-out in the lower die. The first step run-out is mainly used to support the die bearing during the extrusion process, which can effectively prevent the die bearing from invalidation owing to the severe impact between the material and the die bearing. The second step run-out is mainly used to avoid the contact between the die and the extrudate, so that the extrudate could keep away from scratching, until it goes through the die exit successfully. For simplification, the thinner parts, such as the bolt-holes, which are not relevant with simulation, are omitted in the numerical model.

2.2 Numerical simulation model

Figure 3 gives the simulation model for both metal flow and die strength analysis. Being convenient for creating boundary conditions and meshing, the whole model is divided into six parts: billet, porthole and welding chamber, bearing, profile, the lower die, and the upper die. The tri-prism element is adopted in the part of bearing and profile, while

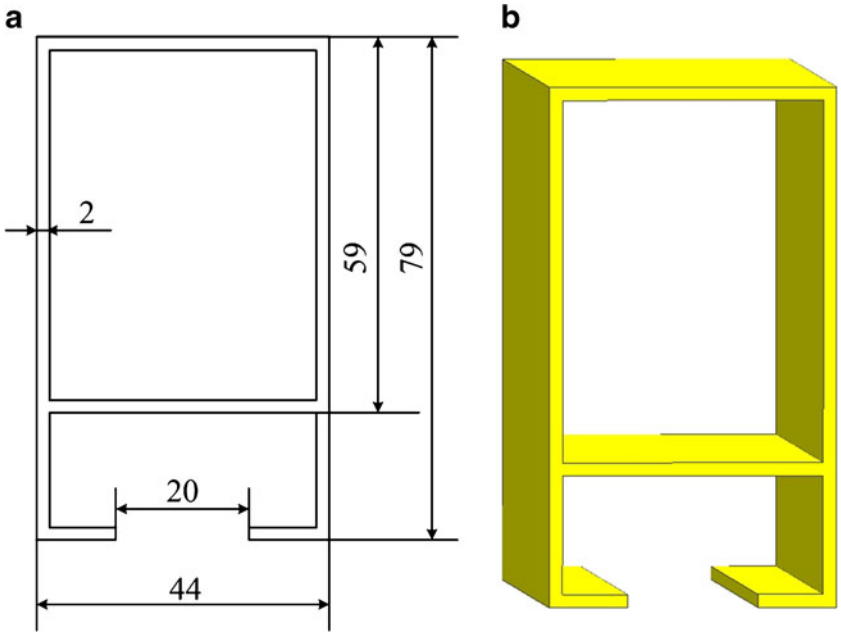

Fig. 1 2D and 3D geometry of the aluminum alloy profile studied in this work: **a** Dimension and geometry of the profile (unit: mm) and **b** 3D model of the profile

tetrahedral element is used in other parts. Moreover, in order to control the element number and ensure calculation accuracy, varying mesh density is adopted in accordance with the extent of local deformation. It should be noted that for die strength analysis with HyperXtrude, the meshes of moving material must be well matched with those of extrusion die in the contact surface except for the bearing, where mismatched contact type is adopted. In the simulation process, AA6063 is used for the billet material with the viscoplastic behavior, while H13 with rigid behavior is used for the extrusion tooling. The material properties of H13 and AA6063 are given in Table 1. The billet used in the simulation is 200 mm in diameter and 400 mm in length, and the calculated extrusion ratio is 60.7. The initial temperature of the billet and the extrusion tooling (including dies and container) are 480 and 460 °C, respectively, and the ram speed is 1 mm/s. In addition, the heat transfer is assumed as heat convection in this work, with the heat convection coefficient of 3,000 W/m^2 °C between the die and billet material. Thus, the simulation model is established in accordance with the above parameters, and its number of element approaches 650,000. The numerical simulation is performed with two Xeon quad processor and 16 G memory workstation and costs about 2 h.

3 Multiobjective optimization design of porthole extrusion die

In this paper, an optimization method based on modern intelligence algorithm is proposed in order to optimize the

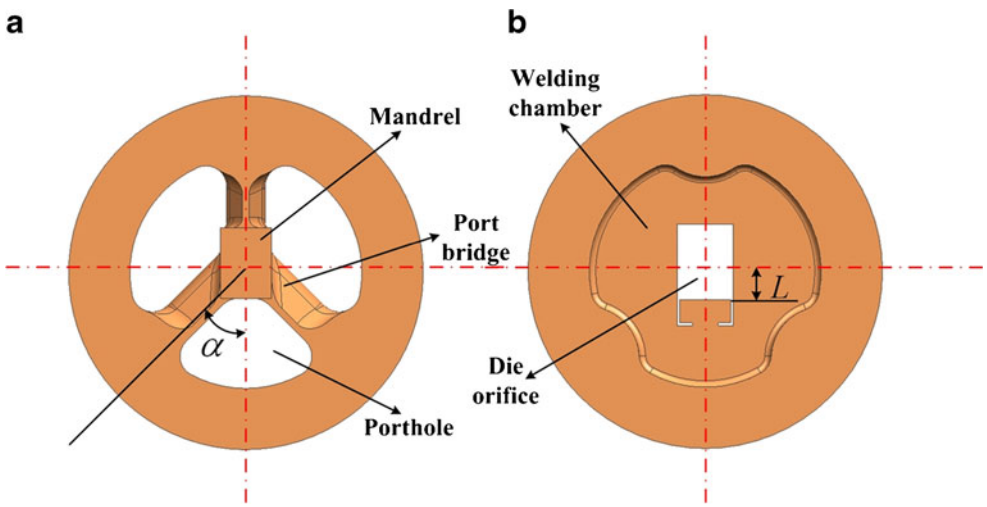

Fig. 2 3D model of the initial porthole die design: **a** upper die and **b** lower die

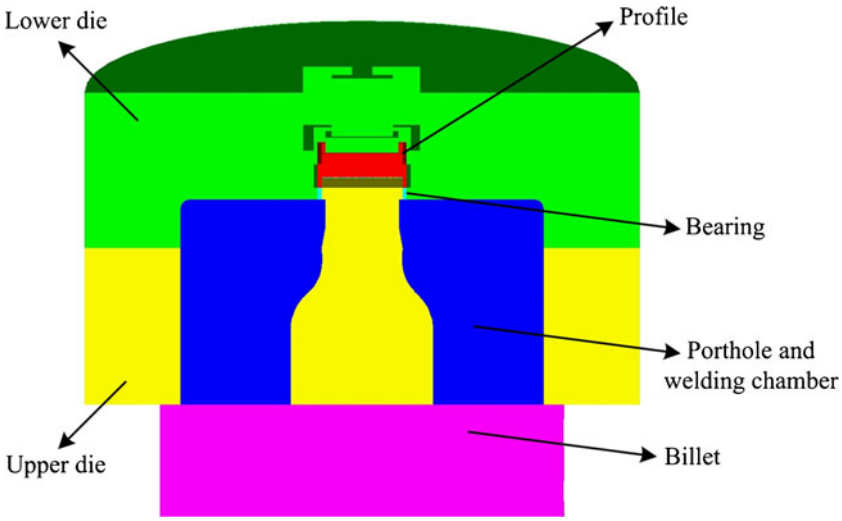

Fig. 3 Simulation model established in this work

porthole die structure. The whole optimization process is composed of five steps: determining design variables and optimization objectives, selecting the sample points, carrying out numerical calculation, establishing Kriging prediction model, and executing Pareto-based genetic algorithm optimization. The flow chart of the optimization process is shown in Fig. 4.

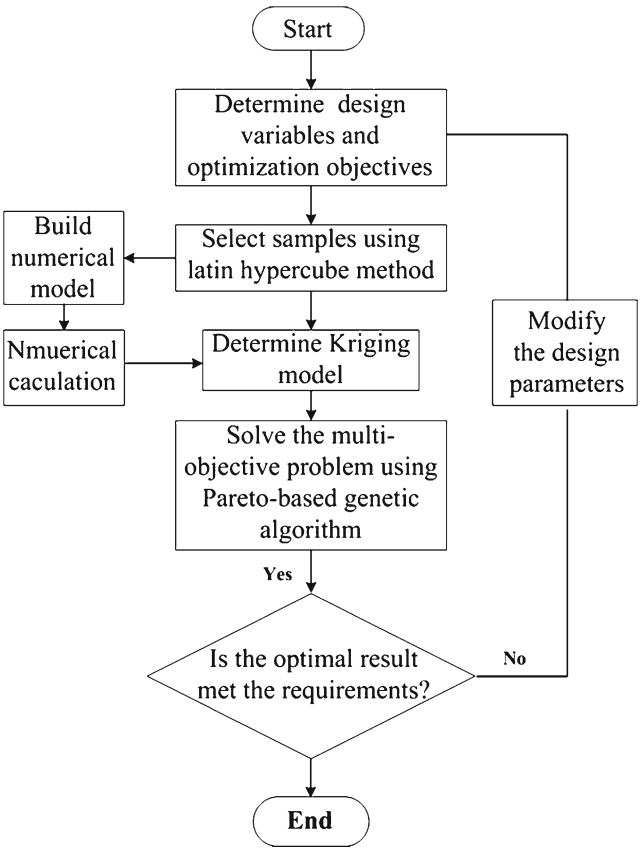

Fig. 4 Flow chart of optimization procedures

3.1 Selection of design variables

The porthole die is mainly composed of six parts: portholes, port bridges, mandrel, welding chamber, die orifice, and run-out. The port bridge is a bracket supporting the die mandrel and influences the extrusion pressure, uniformity of metal flow, weld quality, and die strength directly. With the increasing width and length of port bridge, the die strength would be enhanced, and the extrusion pressure would be increased and vice versa. The die orifice determines the outer features of the profile and has great influence on metal flow and the stress status in extrusion die. The welding chamber is used to collect the material flowing through the portholes and weld them into an integral body again whose center is the die mandrel. When the height of the welding chamber is small, there is not enough welding pressure, so that the metal will not be well-welded. While if the height of the welding chamber is large, the mandrel would be easy to deform, and the extrusion pressure would be increased.

In order to gain an optimal die structure, in this paper, the angle between port bridges(α), the position of die orifice(L), and the height of welding chamber(H) are considered as the design variables in order to gain an optimal die structure. According to practical experience, the ranges of design variables are listed in Table 2.

3.2 Determination of optimization objectives

In real extrusion process, the uniformity of flow velocity distribution in the cross-section of the bearing exit greatly influences the quality of the extrudate. To describe the degree of the velocity uniformity in the cross-section of the extrudate precisely, the function of SDV is introduced in this paper and considered as one optimization objective. The function of SDV is described as follow:

Table 1 Material properties of AA6063 and H13

	Young's modulus/Pa	Poisson's ratio	Density/(Kg m^3)	Thermal conductivity/[N/(s·°C)]	Specify heat/[N/(mm^2·°C)]
AA6063	4.0E+10	0.35	2,700	180	896
H13	2.1E+11	0.35	7,870	24.3	460

$$\mathrm{SDV} = \sqrt{\frac{\sum_{k=1}^{n}\left(v_k - \overline{v}\right)^2}{n}} \tag{1}$$

Where v_k is the velocity at node k in the cross-section to be researched; $\overline{v}$ is the average velocity of all nodes for research; n is the number of nodes to be researched. It is clearly seen that the smaller the SDV values, the better the quality of extruded profile. To show a more practical velocity distribution, in this paper, all nodes in the cross-section of the extrudate are selected for research, of which the velocities are recorded.

During the extrusion process, the extrusion die usually works in a poor environment with high temperature, high pressure, and high friction, which easily causes the porthole die to be early abandoned owing to relatively high stress. Thus, the maximum die stress is selected as the second optimization objective in order to prolong the service life of extrusion die.

The mandrel determines the internal features of the profile; thus, the deflection of mandrel influences the product precision greatly. In general, the deflection of the mandrel in the extrusion direction is compensated by means of increasing the bearing of the mandrel. Here, the maximum deflection of the mandrel in the plane vertical to the extrusion direction is chosen as the third optimization objective, and its value is limited to be less than 0.01 mm.

3.3 Determination of Latin hypercube sampling

In order to represent all the portions of the vector space with limited samples, in this paper, Latin hypercube method is used to determine the experiment scheme. Latin hypercube sampling is a strategy for generating random sample points, ensuring that all portions of the vector space are represented. The Latin hypercube sampling strategy is as follows: (1) Divide the interval of each dimension into umpty non-overlapping intervals having equal probability. (2) Sample randomly from a uniform distribution a point in each interval in each dimension. (3) Pair randomly the point from each dimension. Based on Latin hypercube method, 20 groups of experiment schemes are determined through collocation of three design variables. For each experiment scheme, a new extrusion die was established with corresponding parameters, and the simulation of the extrusion process was executed by means of HyperXtrude. After calculation, the corresponding values such as SDV in the cross-section of the bearing exit, maximum die stress, and mandrel deflection are gained. Table 3 shows the results of all experiment schemes.

Table 2 Ranges of design variables

Design variables	The ranges of design variables
The angle between port bridges α (°)	34 ~ 72
The position of die orifice L (mm)	13.5 ~ 42
The height of welding chamber H (mm)	11 ~ 30

3.4 Establishment of Kriging model

The Kriging model in its basic formulation estimates the value of a function (response) at some unsampled location as a combination of two components, the global model and a systematic departure. Mathematically,

$$Y(x) = f(x)\beta + Z(x) \tag{2}$$

Where $Y(x)$ is the unknown function to be estimated, and the coefficient β is regression parameter. $f(x)$ is a known function (usually a polynomial) representing the trend over the design space, also referred to as the "global model". The second part $Z(x)$ creates a localized deviation to interpolate the sampled data points by quantifying the correlation of points with Gaussian correlation having zero mean and non-zero covariance. The covariance matrix of $Z(x)$ is given by:

$$\mathrm{cov}\left[Z\left(x^i\right), Z\left(x^j\right)\right] = \sigma^2 \mathbf{R}\left[R\left(x^i, x^j\right)\right] \quad i, j = 1, 2, \ldots, n_s \tag{3}$$

Where **R** is a correlation matrix consisting of a spatial correlation function $R(x^i, x^j)$ as its elements. σ^2 is the process variance representing the scalar of the spatial correlation function (SCF) $R(x^i, x^j)$ quantifying the correlation between any two n_s sampled data points x^i, x^j and thereby controls the smoothness of the Kriging model, the effect of nearby points, and differentiability of surface.

The Gaussian function used in the present work is the most preferable SCF when used with a gradient-based optimization algorithm, as it provides a relatively smooth and infinitely differentiable surface. The following Gaussian correlation function is used to obtain the SCF.

Table 3 Latin hypercube sampling

Number	α (°)	*L* (mm)	*H* (mm)	SDV (mm/s)	σ_{max} (Mpa)	dis_{max} (mm)
1	48	27	17	1.30	650.3	0.020
2	66	22.5	27	7.20	622.4	0.045
3	56	36	28	3.79	607.4	0.066
4	40	28.5	20	1.50	653.3	0.042
5	68	34.5	15	3.46	571.1	0.015
6	46	18	12	6.96	703.3	0.016
7	38	30	19	2.27	620.3	0.050
8	58	15	22	11.43	646.2	0.058
9	72	33	23	1.44	595.2	0.008
10	64	16.5	16	12.07	625.5	0.059
11	54	31.5	14	2.27	621.1	0.026
12	34	37.5	29	6.78	651.1	0.109
13	70	19.5	30	11.24	633.7	0.073
14	62	42	18	9.60	542.5	0.069
15	36	39	11	10.52	552.4	0.071
16	52	25.5	21	2.82	678.1	0.015
17	44	40.5	24	8.75	584.7	0.094
18	60	24	25	5.08	642.3	0.021
19	50	21	26	6.39	689.0	0.015
20	42	13.5	13	9.67	710.1	0.025

$$R\left(x^i, x^j\right) = \exp\left[\sum_{k=1}^{n_{dv}} \theta_k \left|x_k^i - x_k^j\right|^2\right] \tag{4}$$

Where n_{dv} is the number of design variables, and θ_k is the unknown correlation parameter used to fit the model [18–21].

For simplicity, in this paper, $f(x)$ is defined as a constant with the value of one. Based on the results in Table 3, the Kriging model between design variables and objective functions is established using Dace toolbox of MATLAB software. The results of Kriging model for response objects are shown in Table 4.

To verify the precision of the Kriging prediction model, in this paper, another five random experiment schemes are selected within the ranges of the design variables, and the numerical result is shown in Table 5. After calculation, the errors between the predicted and numerical results are all less than 10 %. Thus, it illustrates that the result predicted by Kriging model is accurate.

3.5 Execution of Pareto-based genetic algorithm

Generally, although engineering problems include multiple objective optimizations, the objective functions are usually in conflict with each other. That is to say, there is not an optimal design point which can make all the objective functions simultaneously be the best. If a group of parameters is set to optimize the problem with respect to only one objective function, it is possible that the results of the group of parameters will be in opposition to the other objective functions. To be more clear, the Pareto optimal solutions are introduced in the paper. For a minimum value problem, a feasible solution x^* is a Pareto optimal solution, if and only if there is no other feasible solution x such that

$$f_i(x) \le f_i\left(x^*\right) \quad i = 1, \ldots, n \tag{5}$$

And for at least one j, $1 \le j \le n$, satisfying

$$f_j(x) < f_i\left(x^*\right) \tag{6}$$

Table 4 Results of Kriging model for response objects

Objective function	β	θ_1	θ_2	θ_3	σ^2
SDV	0.20	0.21	3.30	0.10	6.78
σ_{max}	−0.097	0.82	0.63	0.16	2160.10
dis_{max}	0.28	0.36	0.82	0.10	0.00061

Table 5 Comparison between Kriging model and numerical simulation

Number	α (°)	*L* (mm)	*H* (mm)	SDV (mm/s)		Error (%)	σ_{max} (Mpa)		Error (%)	dis_{max} (mm)		Error (%)
				Numerical result	Predicted result		Numerical result	Predicted result		Numerical result	Predicted result	
1	36	18	28	2.14	2.34	9.5 %	607.3	618.0	1.8 %	0.015	0.016	8.8 %
2	44	16.5	18	7.53	7.97	5.8 %	725.2	713.9	1.6 %	0.019	0.018	6.7 %
3	56	28	25	2.22	2.14	3.6 %	693.5	673.9	2.8 %	0.023	0.021	9.1 %
4	60	31.5	14	9.57	9.00	6.0 %	597.6	612.5	2.5 %	0.055	0.052	5.8 %
5	68	21	20	6.80	7.03	3.4 %	674.1	696.9	3.4 %	0.024	0.026	7.6 %

To sum up, the Pareto optimal solutions are compromise ones in the feasible solutions region. Every solution would be the best one according to different requirements of the designers, and designer could select the best ones from the Pareto optimal solutions [22–24].

In this paper, the purpose of the optimization is to minimize the SDV in the cross-section of the bearing exit and the maximum die stress. At the same time, the maximum mandrel deflection should be less than 0.01 mm. The optimization problem can be depicted by the following equations:

$$\text{Find}: \alpha, L, H \tag{7}$$

$$\text{Minimize}: \text{SDV}(\alpha, L, H) \text{ and } \sigma_{max}(\alpha, L, H) \tag{8}$$

Subjected to the constraints:

$$dis_{max}(\alpha, L, H) \leq 0.01\,\text{mm} \tag{9}$$

Within ranges:

$$34^\circ \leq \alpha \leq 72^\circ,\ 13.5\,\text{mm} \leq L \leq 42\,\text{mm},\ \text{and}\ 11\,\text{mm} \leq H \leq 30\,\text{mm} \tag{10}$$

The above optimization problem was solved by using nondominated sorting in genetic algorithms (NSGA) based on Pareto combined with Kriging prediction model. NSGA is a computationally efficient algorithm implementing idea of a selection method based on classes of dominance of all the solutions. It incorporates an elitist and a rule for adaptation assignment that takes into account both the rank and the distance of each solution regarding others.

The optimization procedure of NSGA includes the following steps:

1. Encoding parameters. The design variables must be transformed into a form of chromosomes. The chromosomes should contain information about the solutions, which they represent and should be encoded in binary strings.
2. Initializing the population. The individuals which consist of an initial population are produced randomly.
3. Evaluating fitness. The fitness of each individual will be evaluated by objective functions, and Pareto ranking method is used to determine the fitness value. Firstly, setting all individuals initial ranking equal to 1; secondly, evaluating all the individuals by one of the objective functions, and finding individuals whose objective functions value is minimized of all individuals, and set the Pareto ranking of these individuals equal to an integer *k* (the initial value is 1); thirdly, getting rid of these individuals which are equal to *k* and set others equal to *k*+1; then, the previous two steps are continued until all

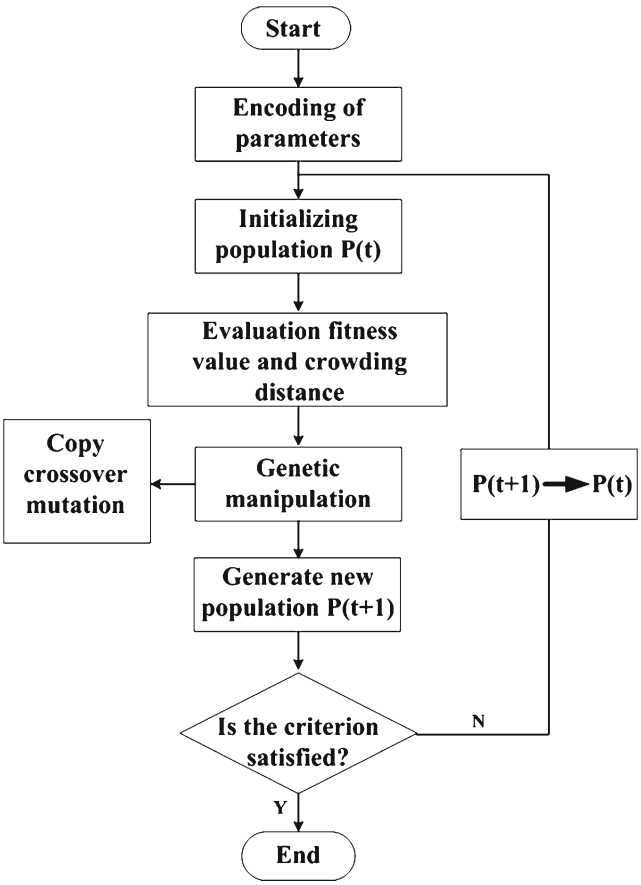

Fig. 5 Flow chart of the multi-genetic algorithm

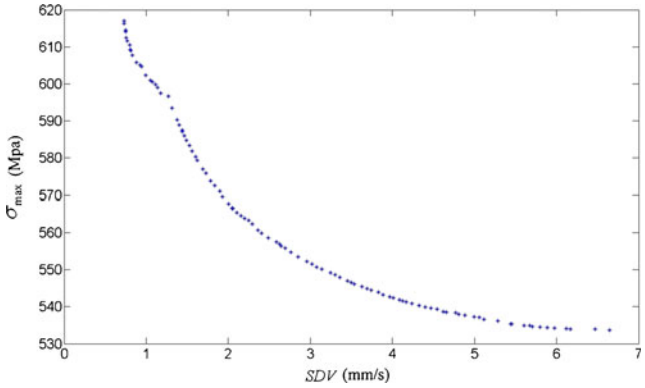

Fig. 6 Pareto optimal solutions of the design variables

of the individuals have their own Pareto ranking. Then the fitness value of each individual is a reciprocal number of their own Pareto ranking.

4. Calculating the crowding distance for each individual. The crowding distance shows how close an individual is to its neighbors. Large average crowding distance will result in better diversity in the population.
5. Genetic manipulation. Parents are selected from the population by using binary tournament selection based on the rank and crowding distance. An individual is selected if the rank is lesser than the other, or if crowding distance is greater than the other. The selected population generates offsprings from crossover and mutation operators (where crossover is a genetic operator used to vary the programming of a chromosome or chromosomes, and mutation is used to maintain genetic diversity from one generation to the next).
6. Termination: Commonly, the algorithm terminates when either a maximum number of generations has been produced, or a satisfactory fitness level has been reached for the population. Otherwise, the process returns to the second step, and all the following steps will be executed again until the termination condition is satisfied [25–29].

The flow chart of multiobjective genetic algorithm is shown in Fig. 5.

In the optimization process, the population size is initialized as 100. The mutation rate is set to 0.01. Uniform crossover is adopted, so that the parent chromosomes could contribute the gene level rather than the segment level, and the crossover rate is set to 0.9. The termination generations are set to 50 in order to save computation time. Figure 6 shows the Pareto optimal solutions of σ_{max} and SDV, which represent the maximum die stress and the SDV in the cross-section of the bearing exit. Each point in the figure represents one Pareto optimal solution. As described above, the smaller the SDV values, the better the quality of extruded profile. While the smaller the maximum die stress σ_{max}, the better the die strength. Therefore, it can be concluded from Fig. 6 that there is a conflicting relationship between the two objectives. When the SDV decreases, the maximum die stress σ_{max} increases and vice versa. Therefore, the best point is selected from 100 groups of Pareto optimal solutions under the limitation that the SDV and σ_{max} should be lesser than 1.5 mm/s and 600 Mpa, respectively. After rounding up, the optimal die structure parameters are gained, where α=71°, L=33 mm, and H=22 mm. Based on the Kriging prediction model, the values of SDV in the cross-section of the extrudate, the maximum die stress, and the maximum mandrel deflection are 1.42 mm/s, 592.7 Mpa, and 0.007 mm, respectively. To verify the predicted result, the confirmation experiment is performed using the optimal die structure parameters by means of HyperXtrude. After calculation, the SDV in the cross-section of the extrudate, the maximum die stress and the maximum mandrel deflection are gained, with the values of 1.36 mm/s, 576.4 Mpa, and 0.008 mm, respectively, which have a small error between estimated and experimental results.

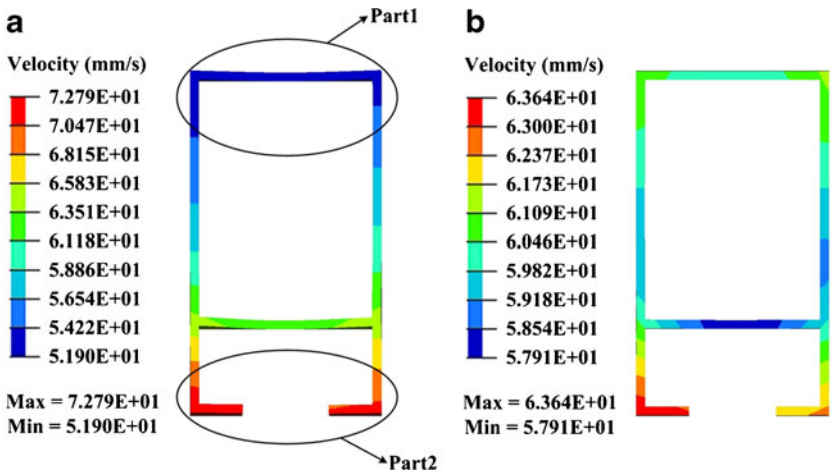

Fig. 7 Comparison of velocity distribution in the cross-section of the extrudate: **a** initial die design and **b** optimal die design

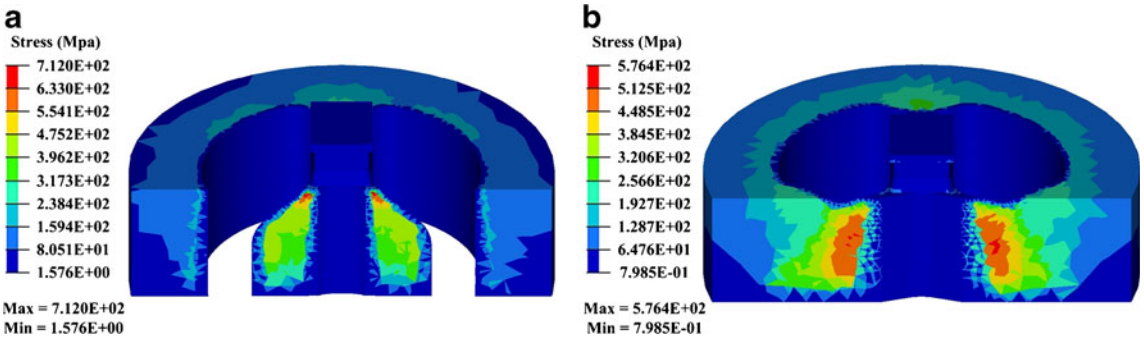

Fig. 8 Comparison of stress distribution in the upper die: **a** initial die design and **b** optimal die design

4 Comparison between the initial and the optimal die design schemes

With the initially designed die structure, the extrusion process simulation is executed in order to compare with the optimal scheme. Figure 7 shows the comparison of velocity distribution at the cross-section of the extrudate for the initial and the optimal scheme. In the initial die design scheme, it is clearly seen that the velocity distribution in the cross-section of the extrudate is not very uniform, and the deflection in four corners of the extrudate is very obvious. The flow velocity in part 2 is faster than that in other parts, and the maximum velocity is up to 72.8 mm/s. The material in part 1 has relatively slower flow velocity, and the minimum velocity is 51.9 mm/s. After calculation, the value of SDV for the initial scheme is up to 6.44 mm/s, and the velocity difference in the extrudate is 21 mm/s. While in the optimal scheme, it is seen that the velocity distribution in the extrudate is very even, and the deflection of the extrudate can be ignored. The maximum velocity is decreased to 63.6 mm/s, and the minimum velocity is increased to 57.9 mm/s. Compared with the initial scheme, the velocity difference between the maximum and minimum velocity and the value of SDV is decreased to 5 and 1.26 mm/s, respectively.

Figure 8 shows the comparison of the stress distribution in the upper die for the initial and the optimal scheme. In both schemes, the maximum stress is observed in the junction of the port bridge and the mandrel, where cracks easily occur. In the initial scheme, the maximum stress in the upper die is 712 Mpa. While in the optimal die structure, the maximum stress is decreased by 19 %, with the value of 576 Mpa; thus, it is favorable to improve service life of extrusion die. In addition, in the optimal scheme, the maximum deflection in the mandrel is decreased from 0.014 mm of the initial die design scheme to 0.008 mm, thus the precision of the internal features of the profile is greatly improved. The comparison of the optimization objective for the initial and the optimal scheme is shown in Table 6.

5 Conclusions

In this paper, the method for porthole die optimization based on modern intelligence algorithm and numerical simulation was proposed in order to provide theoretical guideline for extrusion die design. A profile with irregular shape was taken as an example, and multiobjective optimization for porthole extrusion die was carried out. Through comparing and analyzing the numerical simulation results, the following conclusions are drawn.

1. In porthole extrusion die design, the angle between port bridges, the position of die orifice, and the height of welding chamber are important parameters that influence the product quality and service life of extrusion die directly. Thus, with a properly designed die structure, metal flow could be effectively controlled, and the die stress and the mandrel deflection could be decreased greatly.
2. Through multiobjective optimization of the porthole die, an optimal die structure is gained. With the optimal die structure, the value of SDV in the cross-section of the extrudate is only 1.36 mm/s. The maximum die stress is 576.4 Mpa, and the maximum mandrel deflection is 0.008 mm. Compared with the initial scheme, the above values were decreased by 79, 19, and 47 %, respectively.

Table 6 Comparison of the initial and optimal schemes

	Design variables				Optimization objective	
Parameters	α (°)	L (mm)	H (mm)	SDV (mm/s)	σ_{max} (Mpa)	dis_{max} (mm)
Initial scheme	45	20	25	6.41	712.0	0.014
Optimal scheme	71	33	22	1.36	576.4	0.008

Thus, the profile quality was greatly improved, and the extrusion service life of extrusion die was prolonged.

3. In this paper, the multiobjective optimization design of porthole extrusion die based on CAD, CAE, and CAO has strong commonality, thus, it could be used to solve the multiobjective problem of the same kind profile.

Acknowledgments The authors would like to acknowledge the financial support from the Program for Changjiang Scholars and Innovative Research Team in University of Ministry of Education of China (IRT0931), National Natural Science Foundation of China (51105230), Shandong Provincial Natural Science Foundation (Z2008F09), State Key Laboratory of Materials Processing and Die and Mold Technology (2011-P09), and National Science and Technology Pillar Program in the Eleventh Five-year Plan Period of the People's Republic of China (2009BAG12A07-B01).

References

1. Bauser M, Sauer G, Siegert K (2006) Extrusion, 2nd edn. ASM International, Ohio
2. Liu G, Zhou J, Duszczyk J (2008) FE analysis of metal flow and weld seam formation in a porthole die during the extrusion of a magnesium alloy into a square tube and the effect of ram speed on weld strength. J Mater Process Technol 200:185–198
3. Ceretti E, Fratini L, Gagliardi F, Giardini C (2009) A new approach to study material bonding in extrusion porthole dies. CIRP Ann Manuf Technol 58:259–262
4. Mehtaa BV, Al-Zkeri I, Gunasekera JS, Buijk A (2001) 3D flow analysis inside shear and streamlined extrusion dies for feeder plate design. J Mater Process Technol 113:93–97
5. Wu XH, Zhao GQ, Luan YG, Ma XW (2006) Numerical simulation and die structure optimization of an aluminum rectangular hollow pipe extrusion process. Mater Sci Eng, A 435–436:266–274
6. Chen FK, Chuang WC, Torng S (2008) Finite element analysis of multi-hole extrusion of aluminum alloy tubes. J Mater Process Technol 201:150–155
7. Zhang CS, Zhao GQ, Chen H, Guan YJ, Li HK (2012) Optimization of an aluminum profile extrusion process based on Taguchi's method with S/N analysis. Int J Adv Manuf Technol 60:589–599
8. Fang G, Zhou J, Duszczyk J (2008) Effect of pocket design on metal flow through single-bearing extrusion dies to produce a thin-walled aluminum profile. J Mater Process Technol 199:91–101
9. Wu CY, Hsu YC (2002) Optimal shape design of an extrusion die using polynomial networks and genetic algorithms. Int J Adv Manuf Technol 19:79–87
10. Zou L, Xia JC, Wang XY, Hu GA (2003) Optimization of die profile for improving die life in the hot extrusion process. J Mater Process Technol 142:659–664
11. Li F, Lin JF, Yuan J, Liu XJ (2009) Effect of inner cone punch on metal flow in extrusion process. Int J Adv Manuf Technol 42:489–496
12. Kathirgamanathan P, Neitzert T (2003) Optimization of pocket design to produce a thin shape complex profile. Prod Eng Res Devel 142:231–241
13. Donati L, Tomesani L (2004) The prediction of seam welds quality in aluminum extrusion. J Mater Process Technol 153–154:366–373
14. Arif AFM, Sheikh AK, Qamar SZ, Al-Fuhaid KM (2001) Variation of pressure with ram speed and die profile in hot extrusion of aluminum-6063. Mater Manuf Process 16:701–716
15. Masri K, Warburton A (1996) Optimizing the yield of an extrusion process in the aluminum industry. Lect Notes Econ Math Syst 432:107–115
16. Zhang CS, Zhao GQ, Chen H, Guan YJ, Kou FJ (2012) Numerical simulation and metal flow analysis of hot extrusion process for a complex hollow aluminum profile. Int J Adv Manuf Technol 60:101–110
17. Chitkara NR, Kim YJ (2002) Development of an adaptive directional reduced integration technique and its application to rigid-plastic finite element analysis of heading and backward extrusion. Int J Adv Manuf Technol 20:581–588
18. Sakata S, Ashida F, Tanaka H (2010) Stabilization of parameter estimation for Kriging-based approximation with empirical semivariogram. Comput Methods Appl Mech Eng 199:1710–1721
19. Dellino G, Lino P, Meloril C, Rizzo A (2009) Kriging metamodel management in the design optimization of a CNG injection system. Math Comput Simul 79:2345–2360
20. Lee KD, Kim KY (2011) Surrogate based optimization of a laidback fan-shaped hole for film-cooling. Int J Heat Fluid Flow 32:226–238
21. Verma S, Balaji C (2007) Multiparameter estimation in combined conduction–radiation from a plane parallel participating medium using genetic algorithms. Int J Heat Mass Transf 50:1706–1714
22. Copiello D, Fabbri G (2009) Multiobjective genetic optimization of the heat transfer from longitudinal wavy fins. Int J Heat Mass Transf 52:1167–1176
23. Liu W, Yang YY (2008) Multiobjective optimization of sheet metal forming process using Pareto-based genetic algorithm. J Mater Process Technol 208:499–506
24. Wang XD, Hirsch C, Kang S, Lacor C (2011) Multiobjective optimization of turbomachinery using improved NSGA-II and approximation model. Comput Methods Appl Mech Eng 200:883–895
25. Prakash A, Chan FTS, Deshmukh SG (2011) FMS scheduling with knowledge-based genetic algorithm approach. Expert Syst Appl 38:3161–3171
26. Behroozsarand A, Shafiei S (2011) Multiobjective optimization of reactive distillation with thermal coupling using nondominated sorting genetic algorithm-II. J Nat Gas Sci Eng 3:365–374
27. Kwong CK, Chan KY, Tsim YC (2009) A genetic algorithm-based knowledge discovery system for design of fluid dispensing processes for electronic packaging. Expert Systems with Applications 36:3829–3838
28. Li XP, Zhao GQ, Guan YJ, Ma MX (2010) Multiobjective optimization of heating channels for rapid heating cycle injection mold using Pareto-based genetic algorithm. Polym Adv Technol 21:669–678
29. Kuroki Y, Young GS, Haupt SE (2010) Automatic identification of weather systems from numerical weather prediction data using genetic algorithm. Expert Syst Appl 35:542–555